A novel apparatus and methodology for the high frequency mechanical characterisation of ultra-soft materials

Aaron Graham*, and *Clive R* Siviour

Department of Engineering Science, University of Oxford, Parks Road, Oxford, OX1 3PJ, UK

Abstract. Characterising the mechanical response of ultra-soft materials is challenging, particularly at high strain rates and frequencies [1]. Time Temperature Superposition (TTS) can sometimes be used to mitigate these limitations [2], however not all materials are suitable for TTS. Biological tissues are particularly difficult to test: in addition to the extreme softness, challenges arise due to specimen inhomogeneity, sensitivity to boundary conditions, natural biological variability, and complex post-mortem changes. In the current study, a novel experimental apparatus and methodology was developed and validated using low modulus silicone elastomers as model materials. The full field visco-elastic shear response was characterised over a wide range of deformation frequencies (100-1000+ Hz) and amplitudes using Digital Image Correlation (DIC) and the Virtual Fields Method (VFM). This methodology allows for the extraction of full-field material properties that would be difficult or impossible to obtain using traditional engineering techniques.

1 Introduction

Soft materials have low mechanical stiffness and strength, and include polymers, foams, and biological tissues. Whilst soft materials are widely used in applications where they experience high rate loading, there is a paucity of data on their properties at high strain rates and frequencies when compared to metals and ceramics. A primary reason for this is the challenges inherent in testing soft materials under these loading conditions. A further limitation of standard engineering test methodologies is the assumption of specimen homogeneity: material inhomogeneity or specimen strain localisation is not detected by traditional engineering tests; a form of full field measurement is needed. Furthermore, precise control of specimen boundary conditions is critical when testing soft materials using traditional methods, and any deviation from the assumed deformation state can lead to large errors. Making use of the VFM solves many of the above issues:

1. When using the dynamic VFM, there is no need for the specimen to be under static equilibrium. Instead, the acceleration fields are included in the measurements, and become a help rather than a hindrance in calculating material properties.

* Corresponding author: aaron.graham@eng.ox.ac.uk

2. The VFM can be setup to make fewer assumptions about boundary conditions and stress distributions, reducing the impact of any misalignments or inexact boundary conditions.
3. The VFM can be setup to take advantage of the full-field measurements provided by DIC, and give a full-field measurement of the material properties. This allows for the testing of heterogeneous materials.

This allows for novel test methodologies, where soft, heterogeneous materials can be tested at very high rates. Properties that would be impossible to access using currently existing techniques are directly measured.

2 Apparatus design and VFM theory

The loading device consisted of a torsional pendulum with a tuneable resonant frequency, driven by a pair of programmable smart shakers. This apparatus is capable of applying a (static) preload to specimens in order to simultaneously probe a wide range of static strain amplitudes at the same time as probing oscillatory strains at various frequencies, however this set of experiments did not make use of this capability – only small strains were investigated.

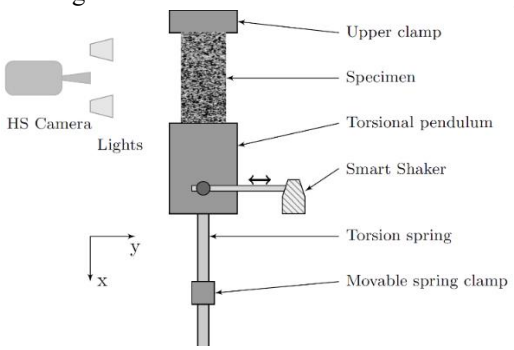

Fig. 1. Apparatus used for loading specimens

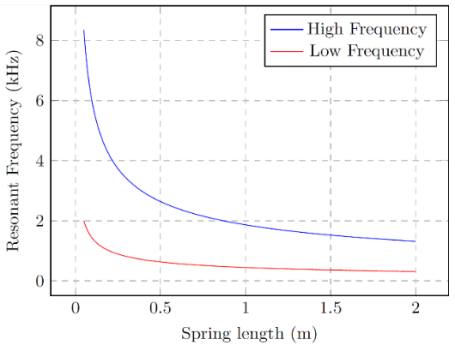

Fig. 2. Range of obtainable resonant frequencies

For each test the specimen was imaged with a Photron FASTCAM SA-X2 1080K-M4 high speed camera at 20 000 fps, with 5000 images taken per frequency.

2.1 Theory

Consider a thin, quasi-1D vertical strip on the specimen shown in Figure 1: If the upper end were unclamped, and the specimen were torsionally loaded, the shear stress distribution down the length of the specimen could be calculated via simple integration of acceleration terms. However, if the end is not free, or if the displacement field over the entire domain is not known, the full VFM is required. The virtual work equation is obtained by multiplying the dynamic equilibrium equation through by a compatible virtual displacement and strain field to give [3]:

$$-\int_V \boldsymbol{\sigma}:\boldsymbol{\epsilon}^*\delta V + \int_{S_f} \boldsymbol{T}\cdot\boldsymbol{u}^*\delta S = \int_V \rho\boldsymbol{u}\cdot\boldsymbol{u}^*\delta V \quad (1)$$

where the first term describes the internal virtual work, the second the external virtual work, and the third describes the virtual work due to acceleration. Appropriate selection of the virtual field can eliminate the traction term, and the acceleration term can be used as a load cell.

First, a virtual displacement field $\boldsymbol{u}^*$ is chosen such that only one unique component of the compatible virtual strain tensor is non-zero. This, in combination with the quasi-1D nature

of the deformation field, allows one to analyse the problem in only one dimension. In 1D linear-elastic shear, with $\boldsymbol{\sigma} = \mu\boldsymbol{\epsilon}$, eq (1) becomes:

$$-\int_{X_0}^{X_1} \mu\boldsymbol{\epsilon}:\boldsymbol{\epsilon}^*\,\delta X - \boldsymbol{T}(X_0)\cdot\boldsymbol{u}^*(X_0) + \boldsymbol{T}(X_1)\cdot\boldsymbol{u}^*(X_1) = \int_{X_0}^{X_1} \rho\ddot{\boldsymbol{u}}\cdot\boldsymbol{u}^*\delta X \tag{2}$$

where X_0 and X_1 are the boundaries of the domain, and μ is the shear modulus. Careful selection of the virtual displacement term allows the traction term to be eliminated from eq (2), resulting in the following expression for the shear modulus:

$$\mu = \frac{\int_{X_0}^{X_1} \rho\ddot{\boldsymbol{u}}\cdot\boldsymbol{u}^*\delta X}{-\int_{X_0}^{X_1} \boldsymbol{\epsilon}:\boldsymbol{\epsilon}^*\delta X} \tag{3}$$

As the primary purpose of these experiments is to investigate the frequency response of soft materials, it is logical to examine the data in the frequency rather than the time domain. A Fast Fourier Transform (FFT) is used to obtain the strain and acceleration data in the frequency domain, in turn allowing for the frequency dependant viscoelastic complex modulus to be solved directly from eq (3):

$$\tilde{G}(f) = G' + iG'' = \frac{\int_{X_0}^{X_1} \rho\tilde{\ddot{\boldsymbol{u}}}(f)\cdot\boldsymbol{u}^*\delta X}{-\int_{X_0}^{X_1} \tilde{\boldsymbol{\epsilon}}(f):\boldsymbol{\epsilon}^*\delta X} \tag{4}$$

Here, both strain and acceleration are complex valued, giving the frequency dependant shear modulus at discrete frequencies. A major advantage of this is the improvement of the signal to noise ratio that results, as the input loading is designed to be a 'pure' frequency, resulting in almost all of the signal for a given test residing on a single frequency band.
For further detail on the above theory, including more in depth derivations and explanations of the requirements for the quasi-1D analysis to be valid, as well as FEA validation of assumptions, the reader is referred to [4].

3 Test methodology

Sylgard 184 is a popular 2 part crosslinked Polydimethylsiloxane (PDMS) material. The material is supplied as a separate base and crosslinker, with a nominal mixing ratio of 10:1 base:crosslinker for full curing [5]. The mechanical properties can easily be varied by reducing the amount of crosslinker. As a result, Sylgard 184 with various crosslinker percentages was tested. The data for two materials is shown in this paper, one with 20% of the recommended crosslinker, and one with 25% of the recommended crosslinker.

Table 1. Materials tested.

Resin:crosslinker ratio	Storage modulus at 0.01 Hz, 20 °C
40:1 (25% of full crosslinker)	11.75 kPa
50:1 (20% of full crosslinker)	4.665 kPa

The uncured material was mixed vigorously, before being vacuum degassed for approximately 5 minutes at 5 kPa (absolute). Specimens were cured for at least double the manufacturer recommended curing time, in order to ensure that all crosslinking had taken place and that the mechanical properties had stabilised. Cure temperature between 25 and 80 °C was found to have no effect on the final elastic properties of the specimen, provided that sufficient time had been given for full crosslinking to take place.

3.1 Low rate tests

Low rate shear data was obtained using an Anton Paar MCR Physical 301 rheometer. This apparatus was nominally capable of testing materials at frequencies up to 100 Hz, but it was found that the data was only reliable up to 10 Hz due to slipping of the loading head occurring

at approximately 50 Hz. Tests were conducted at isothermal frequency sweeps from -20 °C up to 80 °C in steps of 10 °C , allowing for the use of TTS to predict higher rate behaviour.

3.2 High rate tests

Specimens for high rate testing were cast in 30 mm diameter moulds and allowed to fully cure before removal from the mould. The speckle pattern was then applied and allowed to dry before testing of the specimen.
In addition to homogeneous specimens, a 2 part silicone stepped specimen was tested. This specimen was prepared by only filling a mould partway with 25% crosslinked PDMS and allowing it to fully cure. Once the bottom portion was fully cured, 20% crosslinked PDMS was poured into the top portion of the mould and allowed to fully cure. This step change in material served two purposes:

1. It created a specimen with known heterogeneous properties and an extremely steep stiffness gradient at the interface. This allows for the validation of the methodology for heterogeneous specimens.
2. It allowed for the extraction of properties for two materials in a single test. The implications of this are promising, as one could potentially test multiple different soft materials in a single test, greatly reducing the required number of tests

4 Results and comparison to traditional methods

Figure 3 shows the storage moduli of the two materials tested over a range of frequencies and temperatures. Note the somewhat counterintuitive rise in modulus with temperature at low frequencies. This is thought to be as a result of the long term modulus increasing with temperature as expected from the thermodynamics of the system [6]. Unfortunately, this makes TTS challenging, as the isothermal frequency sweeps overlap rather than being parallel.

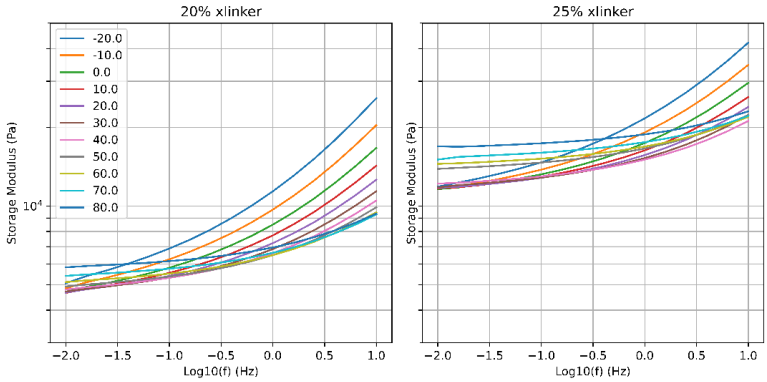

Fig. 3. Storage moduli for isothermal frequency sweeps for Sylgard184 with 20% (left) and 25% (right) of the recommended crosslinker

In order to mitigate this, additional tests were done on the material with 20% crosslinker, recording an additional datapoint at 10^{-3} Hz for each isotherm. This datapoint was assumed to be a measure of G_∞ , which is purely dependant on temperature and not frequency. TTS analysis was then conducted by first stripping the long term moduli from the modulus data, shifting the isotherms, and then adding the long term modulus data back to the TTS data. This is shown in Fig 4, where the plot on the left is the mastercurve generated using this

modified TTS method, whereas the plot on the right is the mastercurve generated using traditional TTS methods.

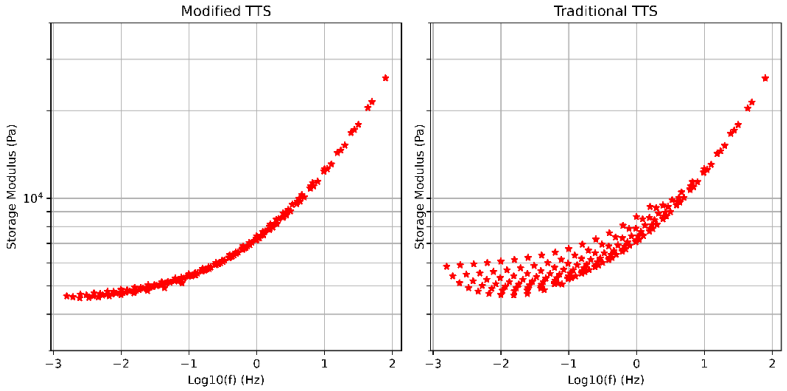

Fig. 4. TTS Mastercurve for Sylgard184 with 20% of recommended crosslinker at 20 ºC. Left, modified TTS. Right, 'traditional' TTS. Note the poor performance of traditional TTS shifting

The downside of this method is the requirement for very low frequency data, which takes a long time to obtain. Additionally, the assumption that data at 10^{-3} Hz is representative of G_∞ is a compromise. Obtaining data at a lower frequency would be more representative of G_∞, but would take substantially longer to obtain. Additionally, it is not clear how valid this approach is, and further experimentation is required.

4.1 High rate data

Figure 5 shows the high rate data obtained for both materials, as well as the low rate data obtained on the rheometer. Only one TTS mastercurve is shown, as the extremely low rate data was only available for the 25% crosslinked material, and this material exhibited significantly greater overlap of the isotherms, further invalidating the traditional TTS process. Note the good fit between the low rate and the high rate data for the material with 20% crosslinker in particular. In addition to validating the high rate data, it further implies that the modified TTS shifting method is valid.

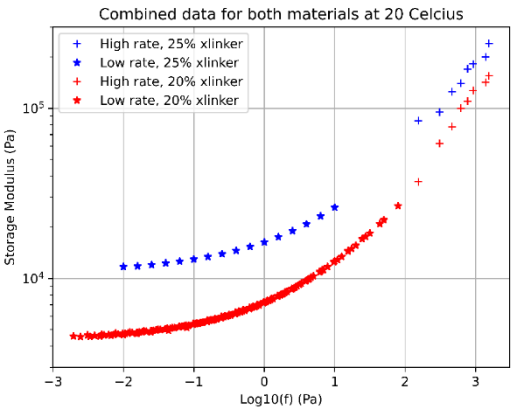

Fig. 5. Combined low and high rate data for both materials at 20 ºC

Figure 6 shows a plot of the spatial distribution of the storage modulus for a heterogeneous sample, where half of the specimen contains material with 20% of the recommended crosslinker, and half of the specimen has 25% of the recommended crosslinker. Note that the obtained moduli closely match the data shown in Fig 5, validating the capability of this apparatus to measure heterogeneous materials. Note however that the measured transition is not instantaneous. This is likely an artefact of the DIC measurement, as DIC is effectively a low pass spatial filter.

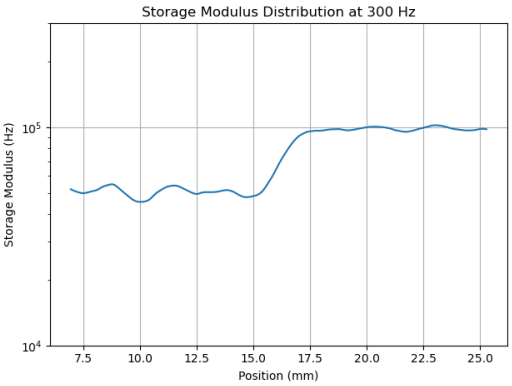

Fig. 6. Spatial distribution of storage modulus at 300Hz, 20 °C

5 Conclusion

This apparatus is capable of accurately characterising the viscoelastic mechanical properties of extremely soft materials at high frequencies. In addition to enabling properties to be measured at high frequencies, properties of heterogeneous materials can be obtained, which cannot be done with traditional methodologies such as rheometry. Whilst TTS can predict the high rate behaviour of some materials via low rate testing, this method is not usable on many materials, such as biological tissue. Unlike TTS, the new methodology does not require experiments at different temperatures, and as such as usable on a far wider range of materials.

6 References

1. W. W. Chen, J. Dyn. Behav. Mat, vol. **2**, pp 2-14, (2016)
2. M. L. Williams, R. F. Landel and J. D. Ferry, J. Am. Chem. Soc, vol. **77**, no 14, pp. 3701-3707, (1955)
3. F. Pierron and M. Grediac, The Virtual Fields Method, New York: Springer New York, (2012)
4. A. Graham and C. Siviour, Strain, https://doi.org/10.1111/str.12386, (2021)
5. K. Khanafer, A. Duprey, M. Schlicht and R. Berguer, Biomed Microdevices, vol. **11**, no.2, pp. 503-508, (2009)
6. W. Kelvin, Quarterly J. Math, vol. **1**, no. 57, (1857)